Article:
Xia, X, Stewart, DI orcid.org/0000-0001-5144-1234, Cheng, L et al. (3 more authors) (2022) Variation of bacterial community and alkane monooxygenase gene abundance in diesel n-alkane contaminated subsurface environment under seasonal water table fluctuation. Journal of Contaminant Hydrology, 248. 104017. ISSN 0169-7722

https://doi.org/10.1016/j.jconhyd.2022.104017

Variation of bacterial community and alkane monooxygenase gene abundance in diesel n-alkane contaminated subsurface environment under seasonal water table fluctuation

Xuefeng Xia [a, c], Douglas Ian Stewart [b], Lirong Cheng [a, c], Yueqiao Liu [a, c], Yingying Wang [a, c], Aizhong Ding [a, c, *]

[a] College of Water Sciences, Beijing Normal University, Beijing 100875, China

[b] School of Civil Engineering, University of Leeds, Leeds LS2 9JT, UK

[c] Engineering Research Center of Groundwater Pollution Control and Remediation, Ministry of Education, Beijing 100875, China

* Corresponding author

E-mail address: ading@bnu.edu.cn (A. Ding).

Full postal address: No. 19, XinJieKouWai St., Haidian District, Beijing 100875, P.R. China.

Abstract

n-Alkanes, the main component of diesel fuel, are common light non-aqueous phase liquids (LNAPLs) that threaten ecological security. The subsurface from vadose zone, through fluctuating zone, to saturated zone, is a critical multi-interface earth layer which significantly affects the biodegradation processes of n-alkanes. A pilot-scale diesel contaminated aquifer column experiment has been undertaken to investigate the variations of bacterial community and alkane monooxygenase (*alkB*) gene abundance in these zones due to water-table fluctuations. The n-alkanes formed a layer immediately above the water table, and when this was raised, they were carried upwards through the fluctuating zone into the vadose zone. Water content and n-alkanes component C10-C12 are main factors influencing bacterial community variation in the vadose zone, while C10-C12 is a key driving factor shaping bacterial community in the fluctuating zone. The most abundant bacterial phyla at all three zones were *Proteobacteria*, *Firmicutes* and *Actinobacteria*, but moisture-niche selection determined their relative abundance. The intermittent wetting cycle resulted in higher abundance of *Proteobacteria*, and lower abundance of *Actinobacteria* in the vadose and fluctuating zones in comparison to the control column with a static water-table. The abundances of the *alkB* gene variants were relatively uniform in different zones, probably because the bacterial populations harboring *alkB* gene are habituated to biogenic n-alkanes rather than responding to diesel fuel contamination. The variation in the bacterial populations with height due to moisture-niche selection had very little effect on the *alkB* gene abundance, possibly

because numerous species in both phyla (*Proteobacteria* and *Actinobacteria*) carry an *alkB* gene variant. Nevertheless, the drop in the water table caused a short-term spike in *alkB* gene abundance in the saturated zone, which is most likely associated with transport of solutes or colloids from the fluctuating zone to bacteria species in the saturated zone, so a fluctuating water table could potentially increase n-alkane biodegradation function.

Keywords: Water-table fluctuations; Moisture; n-Alkane; Bacterial community; Alkane monooxygenase gene

1. Introduction

Petroleum is an important chemical raw material that is widely used to generate energy to support the demands of modern living all over the world (Gkorezis et al., 2016). However, leaks inevitably occur during production, processing, transportation, storage and usage, frequently resulting in contamination of the subsurface environment with petroleum hydrocarbons (Zhu et al., 2017). After petroleum hydrocarbons enter the soil-groundwater system, they will undergo a series of complex physical, chemical and microbiological reaction processes and exhibit composition and concentration changes (Bauer et al., 2008). Many factors affect the environmental behavior of petroleum hydrocarbons, but water-table fluctuations caused by hydrological dynamics, such as rainfall infiltration and regional groundwater extraction (Rühle et al., 2015; Mossmark et

al ., 2008), will have a significant impact on their migration, transformation and redistribution (Dobson et al., 2007; Sinke et al., 1998).

During the water-table fluctuations, a zone of fluctuating saturation is produced between the continuously unsaturated (vadose) zone and continuously saturated zone below the lowest water table (Xia et al., 2020a). Water-table fluctuations promote the migration of petroleum hydrocarbons (Stafford and Rixey, 2011), change the spatial distribution of soil moisture and its corresponding pore air (Haberer et al., 2015), and to some extent cause changes in microbial community diversity and structure (Borer et al., 2018). The response of different microorganisms within a community depends on their ability to adapt to a changing environment. However, selection for adaptability tends to produce microbial communities with greater functional diversity and can result in the co-existence of species that are seemingly adapted to different ecological niches (Pett-Ridge and Firestone, 2005). There have been many studies of the shifts in microbial communities of aquifers with varying water tables, but most have only focused on the fluctuating zone (Rezanezhad et al., 2014; Rühle et al., 2015; van Driezum et al., 2018; Gupta et al., 2020). However, the “vadose zone-fluctuating zone-saturated zone” form a continuum in the vertical direction, and petroleum hydrocarbons, dissolved species and colloidal matter can migrate upward and downward within that continuum as the water table fluctuates. Meanwhile, the bacterial community composition must be zone-specific due to the differences in the geochemistry that persists between the vadose, fluctuating and saturated zones (Xiu et al., 2020; Sheng et al., 2021). Improved understanding of the

78 redistribution of petroleum hydrocarbons and responses of microbial composition and
79 function in different zones may help assess petroleum hydrocarbon natural attenuation
80 and optimize remediation technologies for petroleum leakages.

81 Microorganisms play many crucial roles in the natural attenuation of petroleum
82 hydrocarbons in an aquifer, but adaptation of the microbial community to the prevailing
83 geochemical conditions will determine which degradation pathways are active in which
84 zones of an aquifer (Ning et al., 2018). For n-alkanes, the main component of petroleum
85 hydrocarbons (Gkorezis et al., 2016), bacterial communities harboring alkane
86 monooxygenase genes (*alkB*) can mediate alkane single terminal oxidation which is the
87 most effective pathway of n-alkane aerobic biodegradation (Lee et al., 2021b; Tourova et
88 al., 2016). There are a variety of *alkB* genes that share homologous sequences and encode
89 alkane monooxygenase (Jurelevicius et al., 2013). Among them, the *alk_A*, *alk_R* and
90 *alk_P* genes are three major types of *alkB* genes, which have been identified to degrade
91 different carbon chain lengths of n-alkane. The *alk_R* and *alk_P* genes are more effective
92 with short- and medium-chain n-alkanes from C7-C20, while the *alk_A* gene is more
93 responsible for medium- and long-chain n-alkanes from C13-C44 (Wang et al., 2016; Liu
94 et al, 2018). However, it is currently not known if the spatial and temporal variations in
95 the microbial community within an aquifer affects the distribution of these three genes,
96 and thus the pathway and biodegradation rate in the vadose, fluctuating and saturated
97 zones of an aquifer.

98 Recent developments in molecular technology make it feasible not only to map
99 spatial variations in microbial communities and functional gene abundances, but also to
100 track their temporal variations (Gonzalez et al., 2012). For example, a recent study of a
101 hydrologically dynamic alpine oligotrophic aquifer showed dramatic seasonal decreases
102 in the diversity of microbial communities between the relatively nutrient rich period
103 following recharge by summer rains and the nutrient poor period follow recharge by
104 snow melt-water (Zhou et al., 2012). Separately, it has been shown that the abundances of
105 *alk_A*, *alk_R* and *alk_P* genes in hydrocarbon contaminated soil exhibit diverse changes
106 over time due to different n-alkane contamination level (Liu et al., 2018). However,
107 tracking temporal variations in microbial communities and functional gene abundances is
108 a recent innovation, and little other temporal data has been published on n-alkane
109 contaminated "vadose zone-fluctuating zone-saturated zone" continua. Temporal
110 variations of microbial community structure and *alk_A*, *alk_R* and *alk_P* gene
111 abundances in different zones of an aquifer is still very poorly understood, so the
112 functional roles within, and the ecosystem services provided by a microbial population
113 cannot be identified, and thus the impacts from changing groundwater resource use
114 cannot be predicted (Griebler et al., 2014).
115 In the present study, the main component of petroleum hydrocarbons (n-alkane) was
116 chosen as the targeted contaminant. The variation of environmental characteristics,
117 n-alkane, bacterial community and *alkB* gene abundance in a simulated "vadose
118 zone-fluctuating zone-saturated zone" continuum subjected to seasonal water-table

fluctuations were determined. The spatial patterns of correlation between environmental characteristics, n-alkane and bacterial communities were analyzed, and then the driving factors of shaping bacterial community composition were identified.

2. Materials and methods

2.1. Experiment design

Two nominally identical pilot-scale aquifer columns were established in the Water Sciences laboratory at Beijing Normal University (ambient temperature typically 28 ± 0.5 °C). The columns consist of cylindrical acrylic vessels with a length of 120 cm and an internal diameter of 24 cm (see Fig. 1a). The outer wall of each column was wrapped in black cloth to avoid any light entry. Each column had three lateral ports at depths of 90 cm, 60 cm and 30 cm above the base for dissolved oxygen sensors. The sensors were inserted into the column through a Teflon-lined septum nut. A 0.2 mm stainless mesh screen was laid on the bottom of each column to prevent clogging. The columns were filled with fine-grained natural river sand that was collected for this study from a river floodplain near Cihe (Shijiazhuang, China). The columns were filled to a height of 110 cm using a wet-packing procedure to ensure no entrapment of air bubbles (Xia et al., 2020a). A 4 cm layer of coarse-grained natural river sand also collected from Cihe was placed over the fine river sand, leaving 6 cm of open headspace at the top of the column. The upper surface of the coarse river sand surface was exposed to air to replicate natural conditions. The ends of 16 capillary tubes connected to a single manifold were inserted in

the coarse river sand (distributed evenly over the cross-section) so that simulated rainfall could be introduced at the top of the column. The pretreatment of the river sand is described in the supplementary material, and the initial n-alkane composition of the fine river sand are reported in the Fig. S1.

After packing, the column was drained of water through the bottom drainage port, the dry density was 1.60 g cm^{-3}, and the effective porosity was 0.35. O_2-depleted tap water (before use, the tap water was allowed to stand in an open container for several days to release any free chlorine in the water, before it was sparged with N_2 gas) was then injected from the bottom using a peristaltic pump until the water table reached a position 40 cm above the base of the columns. The water table in both columns was then held static for 10 days.

After 10 days, 90 mL diesel oil obtained from a gas station (China Petroleum) was injected into each column at the water table through three Viton tubes buried in the columns (30 mL through each tube) to simulate subsurface leakage. If this oil had completely saturated the sand, it would have formed a layer approximately 5 mm thick immediately above the water table. The water table in both columns was then maintained for 10 days. The water table was then slowly varied following a pattern representative of rainfall infiltration followed by regional extraction (the RI column), while the water-table in the other column was held static for the entire experiment (the ST column). In the first stage of the RI experiment two episodes of rainfall infiltration were simulated. The water table was raised by 20 cm to 60 cm above the base over a period of 50 h by injecting tap

water into the top of the column using a peristaltic pump (the simulated rainfall was not de-aired) at a flow-rate of 1.06 ml min^{-1} (see the supplementary material), then held static for ~16 days and then raised to 80 cm above the base over a second 50 h period. In the second stage, the water table was held static for ~50 days. In the third stage, representing the impact of regional extraction, the water table was lowered to 60 cm above the base over a period of 50 h by pumping groundwater out of the bottom of the column at a flow-rate of 1.06 ml min^{-1}, held static for ~16 days and then lowered to 40 cm above the base at the same flow-rate. Finally, the water table was held static for 10 days. The intended pattern of the water-table during the first 120 days in the RI experiment can be seen from Fig. 1b. It has similar characteristics to the variations that occur in most agricultural regions of China in response to seasonal rainfall and irrigation. Finally, the water table was held static for an extended period of 90 days to examine whether changes in the bacterial community that resulted from the seasonal water-table fluctuations persisted in the long-term. The process of water-table fluctuations created three vertically-separated zones within the RI column, a continuously saturated zone from 0-40 cm above the base, a zone of fluctuating saturation from 40-80 cm, and a continuously unsaturated (vadose) zone from 80-110 cm.

2.2. In-situ monitoring and sand sampling

The volumetric water contents in the vadose and fluctuating zones were monitored by TDR315L probes (Acclima, USA) that were embedded vertically at depths of about

182 80-100 cm and 50-70 cm above the base, which were connected to a data logger CR300
183 (Campbell, USA). The dissolved oxygen in the vadose, fluctuating and saturated zones
184 were monitored by DP-PSt3 probes (PreSens, Germany) that were installed at depths of
185 90 cm, 60 cm and 30 cm above the base, which were connected to an OXY-10 trace SMA
186 meter (PreSens, Germany).

187 Sand samples from depths of 89-91 cm, 59-61 cm and 29-31 cm above the base
188 were collected after 20, 40, 90, 110, 120 and 210 days (time-points 1-6) using a 120 cm
189 long, 1.25 cm diameter, direct push manual sampler (AMS, USA; further experimental
190 details can be found in the supplementary material). These samples were from the vadose
191 zone (V), fluctuating zone (F) and saturated zone (S), respectively. The sand samples
192 were stored at -20 °C for n-alkane and biological analyses (Jurelevicius et al., 2012; Chen
193 et al., 2018; Patil et al., 2022).

194

195 *2.3. n-Alkane analysis*

196 The protocol for n-alkane extraction and purification from the sand was based on
197 previous studies (Liu et al., 2018). After freeze-drying, approximately 1.0 g of sand
198 sample was spiked with 0.5 mL 1-chlorooctadecane (0.0018 mg/L) as a surrogate
199 standard, then extracted with 10 mL hexane using ultrasound at 80 kHz for 40 min. The
200 supernatant was fractionalized by chromatographic column (details in the supplementary
201 material). The fractions containing n-alkane were reduced to less than 2 mL using rotary
202 evaporation, transferred to a 2 mL vial, evaporated using nitrogen gas flow and then

203 re-dissolved in 1 mL hexane with phenanthrene (0.0004 mg/L) as an internal standard.

204 The n-alkanes were analyzed using gas chromatography with mass spectrometry

205 (GC-MS) (Agilent 6890 gas chromatograph with a 5975C mass-selective detector;

206 Agilent, USA). The GC was equipped with a capillary column (J&W HP-5; J &W

207 Scientific Inc., USA). More details can be found in the supplementary material.

208

209 *2.4. Biological analysis*

210 Total DNA was extracted using PowerSoil DNA Kits (MoBio, USA) in accordance

211 with the manufacturer's instruction. The V3-V4 region of bacterial 16S rRNA gene was

212 amplified by polymerase chain reaction (PCR) using the 338F

213 (5'-ACTCCTACGGGAGGCAGCAG-3') and 806R

214 (5'-GGACTACHVGGGTWTCTAAT-3') primers (details in the supplementary material;

215 Xia et al., 2020b). The purified amplicons were subjected to sequencing on an Illumina

216 MiSeq PE300 sequencer (Illumina, USA) at Allwegene Technology Co., Ltd (Beijing,

217 China) using standard protocols. Raw sequence reads were processed using the QIIME

218 version 1.2.1 (see the supplementary material). Processed reads were assigned to

219 operational defined taxonomic units (OTUs) using USEARCH version 10 (Edgar, 2017),

220 where OTUs were defined by minimum of 97% sequence identity between the putative

221 OTU members. OTUs containing only one read (singletons) were not included in

222 downstream analysis, other OTUs were used to annotate the taxonomic information using

223 the Ribosomal Database Project (RDP) classifier version 2.2 (Wang et al., 2007) against

224 the Silva128 16S rRNA database using a confidence threshold of 70% (Zhang et al.,
225 2020). Mothur version 1.34.4 (Xi et al., 2019) was used to conduct the alpha diversity
226 analysis, including rarefaction, Good's coverage, Observed_species, Chao 1 and Shannon
227 index.

228 Quantitative PCR (qPCR) was used on triplicate sub-samples of each sand sample to
229 measure the abundances of three *alkB* genes (*alk_A*, *alk_R* and *alk_P*) using 2 x Taq
230 MasterMix (CWBio, China). Three separate primer pairs were used for each gene
231 targeted (see Table S3 in the supplementary material; Kuhn et al., 2009; Marchant et al.,
232 2006; Wang et al., 2016). Each reaction mixture contained 10 μL of SYBR® Premix Ex
233 Taq™ II (Tli RNaseH Plus), ROXplus (Takara, China), 0.5 μL each of the forward and
234 reverse primers for the target gene (Table S3), 2 μL of template DNA, and double
235 distilled water to yield a total volume of 20 μL. The PCR protocol was 95 °C for 30 s, 45
236 cycles at 95 °C for 5 s and 60 °C for 40 s. Then, an increase of 0.05 °C s^{-1} from 60 to 99
237 was performed to obtain the melting curve analysis of PCR products. The standard curves
238 were constructed with serial dilutions (10-fold) of quantified plasmid DNA containing the
239 fragment of the *alk_A*, *alk_R* and *alk_P* genes, respectively. The R^2 values for the
240 standard curves exceeded 0.99.

241

242 *2.5. Statistical analysis*

243 Multiple correlation analysis was performed using SPSS software 20.0 (IBM, USA).
244 A p value < 0.05 was considered to indicate statistical significance. Redundancy analysis

245 (RDA) was used to explore the multivariate correlations between water content, dissolved
246 oxygen, n-alkanes and bacterial communities using Canoco 4.5 (Microcomputer Power,
247 USA) via Monte Carlo testing with 999 permutations. The top 10 phyla across all the
248 samples were identified, and their relative abundances in each sample were log (x + 1)
249 transformed for the RDA.
250

251 **3. Results**

252 *3.1. Environmental characteristics*

253 *3.1.1. Water content*

254 In the ST column the volumetric water content at ~50cm above the water table (the
255 vadose zone) gradually increased from 4.7% to 8.0% over the experiment (Fig. 2). At the
256 same location in the RI column, the initial volumetric water content was similar to that in
257 the ST column, but it increased rapidly each time the water table was raised to a
258 maximum value of 34.8% on day 42 (2 days after the water table reached its maximum),
259 but it then decreased while the water table was maintained at its highest level to a value
260 of 27.2%. When water table was lowered to its original level there was an 8-10 day lag in
261 the response of volumetric water content in the vadose zone to each of the two
262 decrements, but it was 13.4% 10 days after the water table was returned to its baseline
263 level and then gradually decreased to 12.2% by the end of the experiment.

264 The volumetric water content at ~20cm above the baseline water table in the ST
265 column (the mid-point of the fluctuating zone in the RI column) gradually decreased

266 from 33.5% to 13.5% over the course of the experiment. At the same location in the RI
267 column the volumetric water content was initially 31.0%, but decreased over the first 20
268 days while the water table was static to 24.2% (introduction of the oil had only a small
269 effect on this trend). The volumetric water content then increased as the water table was
270 raised, to 28.5% when the water table was approximately at the level of the probe, and
271 33.9% when the water table reached its highest level ~20 cm above the probe. The
272 volumetric water content exhibited only minor variations when the water table was static
273 at its highest level. When water table in the RI column was lowered, the response at the
274 mid-height in the fluctuating zone to the first decrement was very small (it decreased to
275 32.7%) and this response lagged ~10 days behind the change in the water table. There
276 was a larger response to the second decrement, with the volumetric water content
277 decreasing rapidly to 25.0% after a lag of ~10 days, before gradually decreasing further
278 to 17.1% by the end of the experiment.
279
280 *3.1.2. Dissolved oxygen*
281 The dissolved oxygen (DO) concentration in the vadose zone exhibited essentially
282 the same response in the RI experiment and the ST control, with the initial value of about
283 8.7 mg L^{-1} (close to equilibrium with atmosphere) gradually decreasing over the course of
284 the experiments to about 7.1 mg L^{-1} (Fig. 3).
285 At the mid-point of the fluctuating zone (~20cm above the baseline water table), the
286 DO concentration in the ST column exhibited essentially the same response as in the

287 vadose zone (it decreased gradually from an initial value of 8.4 mg L^{-1} to 7.0 mg L^{-1} at
288 the end of the experiment). In contrast, the DO concentration in the RI column (initially
289 8.6 mg L^{-1}) remained similar to that value in the vadose zone only for the first ~50 days
290 (the water table was raised to its highest level on day 40), but it then decayed to 0 mg/L
291 over the next ~20 days, and maintained that value until about day 100 (the water table
292 was lowered to roughly the sensor level on day 92). The DO concentration in the
293 fluctuating zone of the RI column then gradually increased to a value of 7.5 mg L^{-1} over a
294 period of 20 day and remained relatively steady at that value for the remaining 90 days of
295 the experiments (Fig. 3).

296 The DO concentration at ~10cm below the baseline water table (the saturated zone)
297 exhibited essentially the same response in the ST and RI columns, with the initial value
298 of ~3.6 mg L^{-1} gradually decreasing to 0 mg/L over a period of ~20 day, and the DO
299 concentrations in the saturated zones of the columns did not increase again during the
300 experiments (Fig. 3).

301

302 *3.2. n-Alkane composition and concentration*

303 The total n-alkane concentration in the RI column and ST control varied with the
304 sampling location relative the baseline water table (see Fig. 4, which also shows the
305 distribution of n-alkanes by alkane chain length). The total n-alkane concentration in the
306 ST control varied principally with position relative to the water table. The time-averaged
307 total n-alkane concentration in the saturated zone 10 cm below the static water table was

12.0 mg/kg, whereas it was 7.1 mg/kg at 20 cm above, and 2.9 mg/kg at 50 cm above the static water table. Whilst these values, which are the average from six time-points, show a consistent trend, it is noted that they are similar in magnitude to the background total n-alkane concentration in the aquifer sand (8.5 mg/kg; see Fig. S1), so the difference may simply reflect natural variability in the sand.

In the RI column, the time-averaged total n-alkane concentration in the fluctuating and vadose zones (10.9 mg/kg and 13.1 mg/kg, respectively) were both generally higher than those in the equivalent zones of the ST control, whereas in the saturated zone it was similar to the ST control (9.7 mg/kg). Also, the total n-alkane concentrations in the RI column exhibited a temporal pattern that can be attributed to the change in the water table. When the water table was raised, the total n-alkane concentration in the saturated and fluctuating zones progressively decreased (from 19.7 mg/kg and 24.5 mg/kg, to 3.0 mg/kg and 4.0 mg/kg, respectively), while the total n-alkane concentration in the vadose zone increased (from 9.4 mg/kg to 28.2 mg/kg). However, the pattern in the total n-alkane concentrations in the RI column was less clear after the water table was lowered again, but total n-alkane concentration in the saturated, fluctuating and vadose zones were all relatively low by the end of the experiment (3.6 mg/kg, 2.2 mg/kg and 2.6 mg/kg, respectively).

327 *3.3. Bacterial community diversity and structure*

328 The alpha diversity analysis indicates that the sequencing depth was sufficient to
329 characterize the variations in the bacterial populations (Fig. S2 and Table S4; the Good's
330 coverage index >0.96 for all populations). Both measures of OTU richness
331 (observed_species and Chao 1 index) indicate that average OTU richness over the
332 duration of the experiments was slightly higher in the RI column than in the ST control at
333 all three locations (Table S4), however this difference may represent replicate variation
334 between the columns as it is present in the first time point before the water table history
335 differed, and does not increase over time.

336 At phylum level, the bacterial populations of the saturated and vadose zones of the
337 ST column exhibited only small variations with time. In samples from the saturated zone
338 about 40% of sequence reads were assigned to the bacterial phylum *Proteobacteria*,
339 nearly a quarter were assigned to *Firmicutes*, and about 15% were assigned to
340 *Actinobacteria* (Fig. 5). Whereas, in samples from the vadose zone <20% of sequence
341 reads were assigned to the bacterial phylum *Proteobacteria*, ~15% were assigned to
342 *Firmicutes*, and nearly half were assigned to *Actinobacteria*. There was more variation
343 between the samples taken from 20 cm above the water table in the ST column (the
344 equivalent zone to fluctuating zone in the RI column) but *Proteobacteria*, *Firmicutes* and
345 *Actinobacteria* were in all cases the three most abundant phyla.

346 The bacterial populations of the saturated zone of the RI column were broadly
347 similar at phylum level to those in the saturated zone of the ST column (i.e.

348 *Proteobacteria*, *Firmicutes* and *Actinobacteria* were the three most abundant phyla),
349 however the proportion of the population assigned to the phylum *Proteobacteria*
350 increased to >60% immediately after simulated rainfall raised the water table, and despite
351 decreasing back to <40% with time and remaining at that level while the water table was
352 lowered, the proportion of the population assigned to *Proteobacteria* increased to >50%
353 in the long-term. After the simulated rainfall raised the water table, the bacterial
354 populations of the vadose zone of the RI column differed markedly (even at phylum level)
355 from those of the vadose zone of the ST column, and were actually more comparable
356 with the bacterial populations of samples taken from 20 cm above the water table in the
357 ST column. Over this period a third of sequences were assigned to *Proteobacteria* and
358 20% were assigned to each of *Firmicutes* and *Actinobacteria* (the proportion that were
359 *proteobacteria* was highest immediately after the simulated rain event). Perhaps
360 surprisingly, the bacterial populations of the fluctuating zone of the RI column remained
361 fairly constant with time despite the period of saturation during the experiment, with
362 about a third of sequences assigned to the phylum *Proteobacteria*, ~20% assigned to
363 *Actinobacteria* and <15% assigned to *Firmicutes*.
364
365 *3.4. Alkane monooxygenase gene abundance*
366 In both the RI and ST columns the abundance of the three *alkB* gene variants
367 generally decreased in the order: *alk_P* > *alk_R* > *alk_A* (Fig. 6).

368 Interestingly, while there were only small variations in the abundance of these genes
369 between the triplicate measurements from the same location (suggesting good analytical
370 repeatability), there were considerable temporal variations in the abundance of each gene
371 at each location. However, despite this temporal variability, there are some patterns to
372 gene abundance. The abundance of the *alk_P* gene generally decreased between sample
373 locations in the order: ST vadose zone > RI vadose zone > ST "fluctuating zone"
374 (equivalent zone of RI fluctuating zone) > RI fluctuating zone > the saturated zones. Thus,
375 the time-averaged abundance of the *alk_P* gene was roughly correlated with the distance
376 of the sample location from the water table, although the differences in the time-averaged
377 abundance of the *alk_P* gene in the ST column were small. The notable exception to this
378 pattern was a very high abundance of the *alk_P* gene in the saturated zone of the RI
379 column immediately after the water table had been lowered. The time-averaged
380 abundance of the *alk_R* gene exhibited a similar pattern with sample locations, and again
381 showed a high abundance in the saturated zone of the RI column only for the single
382 time-point immediately after the water table had been lowered. The abundance of the
383 *alk_A* gene was generally about two orders of magnitude lower than the *alk_P* gene, and
384 it was generally slightly higher in saturated zone than the vadose and fluctuating zones,
385 especially, at the time-point immediately after the water table had been lowered.
386

387 *3.5. Relationship among environmental characteristics, n-alkane, bacterial communities*
388 *and alkane monooxygenase genes*

389 RDA analysis was performed to identify the factors driving temporal variations in
390 bacterial community structure in different zones (Fig. 7). For the vadose zone, the first
391 and second RDA axes explained 52% and 19% of the variance, respectively. The water
392 content had the largest significant effect on the bacterial community ($p = 0.001$),
393 explaining 38% of the community variation (Table S5). The C10-C12 concentration had
394 the second largest significant effect on community variation ($p = 0.038$). Moreover,
395 multiple correlation analysis indicates that the total n-alkane, C10-C12, C17-C20 and
396 C21-C25 concentrations have a significant positive correlation with water content (Table
397 S6). The relative abundance of *Proteobacteria* has a significant positive correlation with
398 water content, whereas the *Actinobacteria* has a significant negative correlation with
399 water content. For the fluctuating zone, the first two axes explained 49% of the variance,
400 and the C10-C12 concentration explained 22% of the community variation ($p = 0.022$).
401 For the saturated zone, the first two axes together explained 55% of the variance. The
402 C21-C25 concentration explained 20% of the community variation but with a lower
403 degree of significance ($p = 0.053$).

404 Multiple correlation analysis also indicates the relationship between the *alkB* genes
405 and dominant phyla, but these are either localized to only one aquifer zone, or suggest a
406 correlation between an *alkB* gene variant and a bacterial phylum that does not contain

genera reported to contain the gene (Table S7), so these correlations are unlikely to indicate causality.

4. Discussion

4.1. Effects of water-table fluctuations on environmental characteristics

Once the static water table was established, there were only minor, relatively slow changes in the geochemical conditions within the ST column. There was a very small gradual increase in the volumetric water content at 50 cm (vadose zone), and a decrease at 20 cm above the water table (the "fluctuating zone"), as a steady state pattern of decreasing volumetric water content with height above the water table was established in the absence of rainfall infiltration (Hou et al., 2019). The DO concentrations in both these unsaturated zones had a slight downward gradient but were at values close to equilibrium with atmospheric O_2 at the laboratory temperature (Patel and Vashi, 2015). In contrast, the DO concentration in the saturated zone decreased steadily from the start of the experiment, reaching zero shortly after time point 1 (when the water table was raised in the RI column), with the injection of the diesel fuel having little impact on the rate of decrease. Thus, the influx of oxygen to the saturated zone was less than the rate of consumption, and the saturated zone was essential anoxic (Xia et al., 2020a). Importantly, from time point 1, the geochemical conditions were essential steady in the ST column.

In contrast, the geochemical conditions in the vadose and fluctuating zones of the RI column varied with the water table. After simulated rainfall, saturation in the vadose zone

peaked at about 80% shortly after the water table reached its highest level but dropped quickly to about 70%. Despite this high degree of saturation, the DO concentration was indistinguishable from that in the equivalent zone of the ST column (i.e. it was close to equilibrium with atmospheric O_2). Saturation decreased again as the water table was lowered, and it was only slightly higher than that in the ST column at the end of the experiment. Saturation in the fluctuating zone of the RI column also reached 80% saturation shortly after the water table reached its highest level, but remained at that level whilst the water table was high, and after a short delay the DO concentration decreased to below the detection limit. This suggests that the remaining pore air in the fluctuating zone is trapped in discrete bubbles (which can persist for significant periods of time in shallow groundwater; McLeod et al., 2015), and as a result the DO consumption by microbial respiration exceeded the rate of diffusion from above (Robinson, 2019; Højberg and Sørensen, 1993). There was less change in the geochemical conditions in the RI column below the initial water table (the DO concentration remained below the detection limit from shortly after time point 1), despite the translation of the simulated rainwater into this zone from the fluctuating zone when the water table was lowered.

4.2. Redistributions of n-alkane caused by water-table fluctuations

Diesel is a light non-aqueous phase liquid (LNAPL), so it will have formed a ~5mm thick layer just above the water table. It is also a non-wetting liquid so negligible capillary rise would be expected and, n-alkanes C10 and above, have negligible solubility

in water. Therefore, the modest concentrations of n-alkanes in the “fluctuating” and vadose zones of the ST column are probably mainly biogenic in origin (produced by plants and associated with the soil organic matter). This assumption is supported by the majority being longer n-alkanes (C17-C25; longer chain length n-alkanes are waxes at or below room temperature (NIST, 2021) and can cause diesel fuel to gel at lower temperatures), whereas, typically, >90% of the n-alkanes in diesel fuel are C10-C17 (Liang et al., 2005). Thus, the time-averaged n-alkane concentrations in these zones of the ST column, which are very similar to the n-alkane concentration in the fine river sand (Fig. S1), represent the typical background levels in the columns.

In the saturated zone of the RI column, the time-averaged total n-alkane concentration was similar to that in the saturated zone of the ST column. However, the time-averaged total n-alkane concentration in the vadose and fluctuating zones were higher than those in the equivalent zones of the ST column. Moreover, when the water table was raised, the total n-alkane concentration in the RI column decreased in the saturated zone, but increased in the fluctuating and vadose zones. Various n-alkane components were significantly and positively correlated with water content in the vadose zone. This suggests that the increase in water content led to increase of n-alkane concentration under water-table fluctuation. Previous studies (Kechavarzi et al., 2005) have also shown that the n-alkanes migrate upwards when the water table rises. This is because diesel is a non-polar liquid, so mineral surfaces were strongly water-wetted (water will have readily displaces diesel from surfaces), and so the diesel layer will have

risen with the water table, although a residual amount may have remained trapped in fine pores or associated with organic matter (Powers et al., 1996).

4.3. Variations in bacterial community during water-table fluctuations

The bacterial communities in the ST column exhibited only small variations with time, but there is a progressive change in bacterial community with increasing height due to the decreasing availability of water, and possibly the increasing availability of oxygen. At all three locations the three most abundant bacterial phyla were *Proteobacteria*, *Actinobacteria* and *Firmicutes*. However, the *Proteobacteria* which were dominant in the saturated zone were less abundant in the vadose zone (~40% and ~20% relative abundance, respectively), whereas *Actinobacteria* which were third most abundant in the saturated zone were dominant in the vadose zone (~15% and ~50% relative abundance, respectively). There was also a slight trend of decreasing *Firmicutes* relative abundance with height (~25% in the saturated zone and ~15% in the vadose zone). At phylum level, the bacterial populations in the "fluctuating zone" were more like those in the saturated zone than those in the vadose zone, suggesting that the availability of water has a bigger impact on the populations than the availability of oxygen (the DO concentration in both the vadose and "fluctuating" zones were close to equilibrium with atmosphere, whereas the saturated zone was anoxic). Similar moisture-niche selection amongst these common soil phyla, with *Actinobacteria* more abundant at low and *Proteobacteria* more abundant at high moisture values, has been observed in fine sandy loam from a semi-arid site

(Evans et al. 2014). Bacterial communities dominated by *Proteobacteria*, *Actinobacteria* and *Firmicutes* are found at other petroleum hydrocarbons contaminated soils (Gao et al., 2014; Lu et al., 2014; Liu et al., 2020), and these populations have been identified as the dominant bacterial phyla with the capability of hydrocarbon metabolism (Smith et al., 2015; Shahi et al., 2016; Yang et al., 2014).

At phylum level, the bacterial community in the saturated zone of the RI column was like that in the saturated zone of the ST column. When averaged over the experiment, the relative abundance of the *Proteobacteria* (~45%) was slightly higher, and the *Firmicutes* (~15%) was slightly lower than in the ST column, but the relative abundance of the *Actinobacteria* was ~15% in the saturated zone of both columns. The modest differences in time-averaged communities between the saturated zones were associated with temporal changes in the population of the RI column associated with movement of the water table. There was an increase in the relative abundance of the *Proteobacteria* and a decrease in the relative abundance of the *Firmicutes* both at the end of the period when simulated rainfall raised the water table and 10 days after simulated regional extraction lowered the water table. It is initially surprising that both raising and lowering the water table resulted in similar shifts in the bacterial populations but the causal process may be the same, as rainfall infiltration results in downward percolation of water through unsaturated soil and contaminated capillary fringe to the edge of the saturated zone, whereas drawdown carries accumulated “rainwater” from the fluctuating zone to the saturated zone. These two processes delivered water bodies with similar geochemistry to

512 the saturated zone, most probably by introducing oxygen into the saturated zone, due to
513 the infiltration of oxygen-containing rainwater and entrapment of oxygen from the
514 fluctuating zone as the water table was decreased. At phylum level, the bacterial
515 communities in the fluctuating and vadose zones of the RI column were obviously
516 different from those in the ST column. Water content was identified as the key factor
517 shaping temporal variations in bacterial community in the vadose zone, and C10-C12 was
518 the driving factor of bacterial community in both the vadose and fluctuating zones.
519 Moreover, they were like that in the saturated zone, although there is a decrease in the
520 average relative abundance of the *Proteobacteria* with height within the column (~35%
521 and ~30% in the fluctuating and vadose zones, respectively), and a very small increase in
522 the relative abundance of the *Actinobacteria* (~20% in both the fluctuating and vadose
523 zones). Thus, the higher average water content at both locations due to the variation in the
524 water table moderated the moisture-niche selective pressure that favoured *Proteobacteria*
525 species (Evans et al. 2014). Also, the general similarity of the bacterial populations in the
526 three zones may be an indication that fluctuations in the water table reduce the
527 hydrological and geochemical differences between saturated, fluctuating and vadose
528 zones, and smears the hydrocarbons between the zones, leading to less difference in
529 bacterial habitats provided (Hamamura et al., 2013).
530

531 *4.4. Variations in abundance of alkane monooxygenase gene during water-table*
532 *fluctuations*

533 Bacterial degradation of n-alkanes can occur under both aerobic and anaerobic
534 conditions but is much faster under aerobic conditions (Widdel and Rabus, 2001; Kloos
535 et al., 2006). The alkane monooxygenase (a rubredoxin dependent enzyme; Kloos et al.,
536 2006) has been shown to be a key enzyme in the degradation of n-alkanes in aerobic
537 systems (Jurelevicius et al., 2013; McKenna and Coon, 1970). Three variants of the *alkB*
538 gene that encodes the enzyme alkane monooxygenase were tracked in the column
539 experiments. These variants have been identified in the genome of hundreds of different
540 bacterial species primarily from phyla *Proteobacteria*, *Actinobacteria*, *Bacteroidetes*,
541 *Acidobacteria* and *Spirochaetes* (Jurelevicius et al., 2013; Yakimov et al., 2004; Wentzel
542 et al., 2007; Kim et al., 2021; Nie et al., 2014). In each zone of both the ST and RI
543 columns the abundance of three variants decreased in the order *alk_P* > *alk_R* > *alk_A* (in
544 just one of the 36 samples *alk_A* was slightly more abundant than *alk_R*) and, overall,
545 *alk_P* was ~1000x more abundant than *alk_A*.

546 In the ST column, the time-averaged gene abundances show only modest differences
547 with height in the column. Further, there is no clear temporal pattern in the gene
548 abundances in the fluctuating and vadose zones of this column. Given that soil organic
549 matter usually contains low levels of n-alkanes from plants, these are probably the
550 background abundances of the *alkB* gene variants in the bacterial populations of the soil.
551 However, the abundance of all three gene variants exhibited a similar temporal pattern in

552 the saturated zone of the ST column. First there was an increase in gene variant
553 abundance between time points 1 and 2, then a decrease until time point 4, and only
554 minor variations thereafter. The initial increase in gene abundance may have been a
555 response to the introduction of the diesel while the pore water still contained low levels
556 of dissolved oxygen, followed by a decrease in gene abundances once the system was
557 fully anoxic (Thapa et al., 2012).

558 In the vadose zone of the RI column, the time-averaged abundances of all three gene
559 variants were similar to the mean value in the ST column, whereas in the fluctuating zone
560 they were slightly lower. In the saturated zone of the RI column, the time-averaged
561 abundances of all three gene variants were an order of magnitude higher than the mean
562 value in the ST column. However, this difference is associated with a >100x increase in
563 the abundance of all three gene variants when the water table was lowered from its
564 highest position (time point 4), which was then not sustained once the water table was
565 stable in its lower position. If time point 4 is ignored, the time-averaged abundances of all
566 three gene variants in the saturated zone of the RI column were similar to the mean value
567 in the ST column. Thus, without spike when the water table was lowered, the
568 time-averaged abundances of all three gene variants were very similar in the equivalent
569 zones of the RI and ST columns. The increase in *alkB* gene variants in the saturated zone
570 when the water table was lowered is most likely associated with transport of solutes or
571 colloids from the fluctuating zone to bacteria species in saturated zone, but it is unclear
572 what that species might be (trace dissolved oxygen, dissolved organic matter, nutrients,

573 etc.). However, rapid changes in the bacterial community in the saturated zone due to
574 infiltration of geochemically different water has been observed in other systems (Fillinger
575 et al., 2021).
576

577 *4.5. Implications of the alkane monooxygenase gene distribution*

578 While elevated alkane concentrations in the subsurface environment are usually the
579 result of contamination with petroleum hydrocarbons (Rojo, 2009), alkanes are also
580 produced by many living organisms such as plants and cyanobacteria and form part of the
581 biomass in soil (Bush and McInerney, 2013; Blumer et al., 1971; Schirmer et al., 2010;
582 Kloos et al., 2006). As a result, alkanes are present at low concentrations in most soil and
583 water environments (Brassell et al., 1978; Lee et al., 2021a). This is why
584 alkane-degrading microorganisms are ubiquitous in nature (Wentzel et al., 2007). It is
585 also why the abundance of the *alkB* gene variants was relatively uniform in the columns
586 reported here (with the exception of the RI column after the water table was lowered).
587 This suggests that the introduction of the diesel fuel into the columns generally had very
588 little effect on the *alkB* gene abundance, probably because the bacterial populations
589 harboring *alkB* gene were habituated to biogenic alkanes associated with the soil organic
590 matter, and the abundances of bacteria carrying this gene were limited by factors other
591 than the n-alkane concentration. More surprisingly, the variation in the bacterial
592 populations with height due to moisture-niche selection (with *Actinobacteria* more

593 abundant at low and *Proteobacteria* more abundant at high moisture values) also had
594 very little effect on the *alkB* gene abundance, possibly because numerous species in both
595 phyla carry one or other *alkB* gene variant (Table S7 and references therein).
596 Whilst there was little spatial variation in the abundance of the *alkB* gene variants
597 despite differences in the bacterial populations with height in the column, suggesting that
598 moisture-niche selection does not affect the *alkB* gene abundance, there was a dramatic
599 (100x) increase in the abundance of all three *alkB* gene variants in the saturated zone of
600 the RI column after the water table was lowered. This was not directly associated with
601 transfer of bacteria from a zone where the *alkB* gene abundance was high (*alkB* gene
602 abundance was not higher in the fluctuating zone), or with an increase the n-alkane
603 concentration, so it is inferred that it associated with some other factor affecting the
604 growth of bacteria carrying the *alkB* gene. This may be associated with the transport of a
605 limiting factor to the saturated zone (trace dissolved oxygen, organic matter, nutrients,
606 etc.) or, equally, may have been the result of mixing due to the water flow (n-alkanes are
607 largely insoluble but reaction with a cell-surface-associated oxygenase requires cell
608 contact (Wentzel et al., 2007), so flow-induced mixing may be an important factor).
609 Whatever the cause, it clearly demonstrates that a varying water table can significantly
610 impact on the genetic potential to degrade n-alkane in a system representative of a
611 shallow unconfined aquifer.
612

5. Conclusions

This study proposed that the "vadose zone-fluctuating zone-saturated zone" in a soil column must be considered as a continuum. It reports the spatio-temporal distribution of bacterial community and *alkB* gene abundance in a simulated diesel fuel (LNAPL) contaminated aquifer during water-table fluctuations (*alkB* is an important gene for bacterial degradation of n-alkanes, the main component of diesel fuel). It found by RDA analysis that water content and n-alkanes C10-C12 were the driver of temporal distribution of community structure in the vadose zone, and C10-C12 was the driver of temporal distribution of community structure in the fluctuating zones. Meanwhile, the community structure in the saturated zone shared a similar temporal trend with that in the static condition. We found that moisture-niches selection accounted for the vertical distribution of community structure in subsurface, with relative abundance of *Proteobacteria* increasing, and *Actinobacteria* decreasing with water content, but seasonal water-table fluctuations led to less difference between different zones in the continuum.

The abundances of the *alkB* gene variants were relatively uniform in different zones. However, variation in the water table caused a short-term spike in *alkB* gene abundance in the saturated zone after the water table was lowered, suggesting a fluctuating water table could increase functional potential to degrade n-alkane in the shallow phreatic aquifer.

Declarations of competing interest

None.

Acknowledgments

This work was supported by the National Key R & D Program of China [grant number 2018YFC1800905] and Key Science and Technology Projects of Inner Mongolia Autonomous Region [grant number 2019ZD001].

References

Bauer, R.D., Maloszewski, P., Zhang, Y.C., Meckenstock, R.U., Griebler, C., 2008. Mixing-controlled biodegradation in a toluene plume - Results from two-dimensional laboratory experiments. J. Contam. Hydrol. 96, 150-168.

Blumer, M., Gullard, R.R.L., Chase, T., 1971. Hydrocarbons of marine phytoplankton. Mar. Biol. 8, 183-189.

Borer, B., Tecon, R., Or, D., 2018. Spatial organization of bacterial populations in response to oxygen and carbon counter-gradients in pore networks. Nat. Commun. 9, 769.

Brassell, S.C., Eglinton, G., Maxwell, J.R., Philp R.P., 1978. Natural background of alkanes in the aquatic environment. In: Hutzinger, O., van Lelyveld, L.H., Zoeteman B.C.J. (Eds.), Aquatic Pollutants: Transformation and Biological Effects, Pergamon, Oxford, pp. 69-86.

Bush, R.T., McInerney, F.A., 2013. Leaf wax n-alkane distributions in and across modern plants: Implications for paleoecology and chemotaxonomy. Geochim. Cosmochim. Ac. 117, 161-179.

Chen, Z.Q., Wang, Y., Wen, Q.X., 2018. Effects of chlortetracycline on the fate of multi-antibiotic resistance genes and the microbial community during swine manure composting. Environ. Pollut. 237, 977-987.

Dobson, R., Schroth, M.H., Zeyer, J., 2007. Effect of water-table fluctuation on dissolution and biodegradation of a multi-component, light nonaqueous-phase liquid. J. Contam. Hydrol. 94, 235-248.

Edgar, R.C., 2017. SEARCH_16S: a new algorithm for identifying 16S ribosomal RNA genes in contigs and chromosomes. bioRxiv 124131.

Evans, S.E., Wallenstein, M.D., Burke, I.C., 2014. Is bacterial moisture niche a good predictor of shifts in community composition under long-term drought? Ecology 95, 110-122.

Fillinger, L., Hug, K., Griebler, C., 2021. Aquifer recharge viewed through the lens of microbial community ecology: initial disturbance response, and impacts of species sorting versus mass effects on microbial community assembly in groundwater during riverbank filtration. Water Res. 189, 116631.

Gao, Y.C., Guo, S.H., Wang, J.N., Li, D., Wang, H., Zeng, D.H., 2014. Effects of different remediation treatments on crude oil contaminated saline soil. Chemosphere 117, 486-493.

676 Gkorezis, P., Daghio, M., Franzetti, A., van Hamme, J.D., Sillen, W., Vangronsveld, J.,
677 2016. The interaction between plants and bacteria in the remediation of petroleum
678 hydrocarbons: an environmental perspective. Front. Microbiol. 7, 1836.
679 Gonzalez, A., King, A., Robeson, M.S.II, Song, S., Shade, A., Metcalf, J.L., Knight, R.,
680 2012. Characterizing microbial communities through space and time. Curr. Opin.
681 Biotechnol. 23, 431-436.
682 Griebler, C., Malard, F., Lefebure, T., 2014. Current developments in groundwater
683 ecology-from biodiversity to ecosystem functioning and services. Curr. Opin.
684 Biotechnol. 27, 159-167.
685 Gupta, P.K., Gharedaghloo, B., Lynch, M., Cheng, J.J., Strack, M., Charles, T.C., Price,
686 J.S., 2020. Dynamics of microbial populations and diversity in NAPL contaminated
687 peat soil under varying water table conditions. Environ. Res. 191, 110167.
688 Haberer, C.M., Roy, J.W., Smith, J.E., 2015. Patterns of entrapped air dissolution in a
689 two-dimensional pilot-scale synthetic aquifer. Groundwater 53, 271-281.
690 Hamamura, N., Ward, D.M., Inskeep, W.P., 2013. Effects of petroleum mixture types on
691 soil bacterial population dynamics associated with the biodegradation of
692 hydrocarbons in soil environments. FEMS Microbiol. Ecol. 85, 168-178.
693 Højberg, O., Sørensen, J., 1993. Microgradients of microbial oxygen consumption in a
694 barley rhizosphere model system. Appl. Environ. Microbiol. 59, 431-437.

695 Hou, X.K., Li, T.L., Vanapalli, S.K., Xi, Y., 2019. Water percolation in a thick unsaturated
696 loess layer considering the ground-atmosphere interaction. Hydrol. Process. 33,
697 794-802.
698 Jurelevicius, D., Alvarez, V.M., Peixoto, R., Rosado, A.S., Seldin, L., 2013. The use of a
699 combination of *alkB* primers to better characterize the distribution of
700 alkane-degrading bacteria. PLoS ONE 8, e66565.
701 Jurelevicius, D., Cotta, S.R., Peixoto, R., Rosado, A.S., Seldin, L., 2012. Distribution of
702 alkane-degrading bacterial communities in soils from King George Island, Maritime
703 Antarctic. EUR. J. Soil Biol. 51, 37-44.
704 Kechavarzi, C., Soga, K., Illangasekare, T.H., 2005. Two-dimensional laboratory
705 simulation of LNAPL infiltration and redistribution in the vadose zone J. Contam.
706 Hydrol. 76, 211-233.
707 Kim, N.K., Lee, S.H., Yoon, H., Jeong, G., Jung, Y.J., Hur, M., Lee, B.H., Park, H.D.,
708 2021. Microbiome degrading linear alkylbenzene sulfonate in activated sludge. J.
709 Hazard. Mater. 418, 126365.
710 Kloos, K., Munch, J.C., Schloter, M., 2006. A new method for the detection of
711 alkane-monooxygenase homologous genes (*alkB*) in soils based on
712 PCR-hybridization. J. Microbiol. Meth. 66, 486-496.
713 Kuhn, E., Bellicanta, G.S., Pellizari, V.H., 2009. New alk genes detected in Antarctic
714 marine sediments. Environ. Microbiol. 11, 669-673.

715 Lee, D.H., Kim, J.H., Shin, K.H., 2021a. Application of column chromatography for
716 accurate determination of the carbon isotopic compositions of n-alkanes in diverse
717 environmental samples. Ocean Sci. J. 56, 46-54.
718 Lee, Y.Y., Seo, Y., Ha, M., Lee, J., Yang, H., Cho, K.S., 2021b. Evaluation of
719 rhizoremediation and methane emission in diesel-contaminated soil cultivated with
720 tall fescue (*Festuca arundinacea*). Environ. Res. 194, 110606.
721 Liang, F.Y., Lu, M.M., Keener, T.C., Liu, Z.F., Khang, S.J., 2005. The organic
722 composition of diesel particulate matter, diesel fuel and engine oil of a non-road
723 diesel generator. J. Environ. Monit. 7, 983-988.
724 Liu, H., Gao, H., Wu, M., Ma, C., Wu, J., Ye, X., 2020. Distribution characteristics of
725 bacterial communities and hydrocarbon degradation dynamics during the
726 remediation of petroleum-contaminated soil by enhancing moisture content. Microb.
727 Ecol. 80, 202-211.
728 Liu, Y.Q., Ding, A.Z., Sun, Y.J., Xia, X.F., Zhang, D.Y., 2018. Impacts of n-alkane
729 concentration on soil bacterial community structure and alkane monooxygenase
730 genes abundance during bioremediation processes. Front. Environ. Sci. Eng. 12, 3.
731 Lu, L., Huggins, T., Jin, S., Zuo, Y., Ren, Z.J., 2014. Microbial metabolism and
732 community structure in response to bioelectrochemically enhanced remediation of
733 petroleum hydrocarbon-contaminated soil. Environ. Sci. Technol. 48, 4021-4029.

734 Marchant, R., Sharkey, F.H., Banat, I.M., Rahman, T.J., Perfumo, A., 2006. The
735 degradation of n-hexadecane in soil by thermophilic geobacilli. FEMS Microbiol.
736 Ecol. 56, 44-54.
737 McKenna, E.J., Coon, M.J., 1970. Enzymatic omega-oxidation. IV. Purification and
738 properties of the omega-hydroxylase of *Pseudomonas oleovorans*. J. Biol. Chem.
739 245, 3882-3889.
740 McLeod, H.C., Roy, J.W., Smith, J.E., 2015. Patterns of entrapped air dissolution in a
741 two-dimensional pilot-scale synthetic aquifer. Groundwater 53, 271-281.
742 Mossmark, F., Hultberg, H., Ericsson, L.O., 2008. Recovery from groundwater extraction
743 in a small catchment area with crystalline bedrock and thin soil cover in Sweden. Sci.
744 Total Environ. 404, 253-261.
745 Nie, Y., Chi, C.Q., Fang, H., Liang, J.L., Lu, S.L., Lai, G.L., Tang, Y.Q., Wu, X.L., 2014.
746 Diverse alkane hydroxylase genes in microorganisms and environments. Sci. Rep. 4,
747 4968.
748 Ning, Z., Zhang, M., He, Z., Cai, P.P, Guo, C.J., Wang, P., 2018. Spatial pattern of
749 bacterial community diversity formed in different groundwater field corresponding
750 to electron donors and acceptors distributions at a petroleum-contaminated site.
751 Water 10, 842.
752 NIST Chemistry WebBook, SRD 69. Accessed November 2021.
753 https://webbook.nist.gov/cgi/cbook.cgi?ID=C593453&Units=SI&Mask=FFF#.

Patel, H., Vashi, R.T., 2015. Characterization of textile wastewater. In: Patel, H., Vashi, R.T. (Eds.), Characterization and Treatment of Textile Wastewater. Elsevier, Amsterdam, Netherlands, pp. 21-71.

Patil, M.P., Woo, H.E., Kim, J.O., Kim, K., 2022. Field study on short-term changes in benthic environment and benthic microbial communities using pyrolyzed oyster shells. Sci. Total Environ. 824, 153891.

Pett-Ridge, J., Firestone, M.K., 2005. Redox fluctuation structures microbial communities in a wet tropical soil. Appl. Environ. Microbiol. 71, 6998-7007.

Powers, S.E., Anckner, W.H., Seacord, T.F., 1996. Wettability of NAPL-contaminated sands. J. Environ. Eng. 122, 889-896.

Rezanezhad, F., Couture, R.M., Kovac, R., O'Connell, D., van Cappellen, P., 2014. Water table fluctuations and soil biogeochemistry: an experimental approach using an automated soil column system. J. Hydrol. 509, 245-256.

Robinson, C., 2019. Microbial respiration, the engine of ocean deoxygenation. Front. Mar. Sci. 5, 533.

Rojo, F., 2009. Degradation of alkanes by bacteria. Environ. Microbiol. 11, 2477-2490.

Rühle, F.A., Von Netzer, F., Lueders, T., Stumpp, C., 2015. Response of transport parameters and sediment microbiota to water table fluctuations in laboratory columns. Vadose Zone J. 14, 12.

Schirmer, A., Rude, M.A., Li. X.Z, Popova, E., del Cardayre, S.B., 2010. Microbial biosynthesis of alkanes. Science 329, 559-562.

775 Shahi, A., Aydin, S., Ince, B., Ince, O., 2016. Reconstruction of bacterial community
776 structure and variation for enhanced petroleum hydrocarbons degradation through
777 biostimulation of oil contaminated soil. Chem. Eng. J. 306, 60-66.
778 Sheng, Y.Z., Li, G.H., Dong, H.L., Liu, Y.F., Ma, L., Yang, M.Q., Liu, Y., Liu, J., Deng,
779 S.Q., Zhang, D.Y., 2021. Distinct assembly processes shape bacterial communities
780 along unsaturated, groundwater fluctuated, and saturated zones. Sci. Total Environ.
781 761, 143303.
782 Sinke, A.J.C., Dury, O., Zobrist, J., 1998. Effects of a fluctuating water table: column
783 study on redox dynamics and fate of some organic pollutants. J. Contam. Hydrol. 33,
784 231-246.
785 Smith, E., Thavamani, P., Ramadass, K., Naidu, R., Srivastava, P., Megharaj, M., 2015.
786 Remediation trials for hydrocarbon-contaminated soils in arid environments:
787 Evaluation of bioslurry and biopiling techniques. Int. Biodeter. Biodegr. 101, 56-65.
788 Stafford, B.P., Rixey, W.G., 2011. Distribution of fuel-grade ethanol near a dynamic water
789 table. Ground Water Monit. Remediat. 31, 55-60.
790 Thapa, B., KC, A.K., Ghimire, A., 2012. A review on bioremediation of petroleum
791 hydrocarbon contamination in soil. Kathmandu Univ. J. Sci. Eng. Technol., 8,
792 164-170.
793 Tourova, T.P., Sokolova, D.S., Semenova, E.M., Shumkova, E.S., Korshunova, A.V.,
794 Babich, T.L., Poltaraus, A.B., Nazina, T.N., 2016. Detection of n-alkane

795 biodegradation genes *alkB* and *ladA* in thermophilic hydrocarbon-oxidizing bacteria
796 of the genera *Aeribacillus* and *Geobacillus*. Microbiology 85, 693-707.
797 van Driezum, I.H., Chik, A.H.S., Jakwerth, S., Lindner, G., Farnleitner, A.H., Sommer, R.,
798 Blaschke, A.P., Kirschner, A.K.T., 2018. Spatiotemporal analysis of bacterial
799 biomass and activity to understand surface and groundwater interactions in a highly
800 dynamic riverbank filtration system. Sci. Total Environ. 627, 450-461.
801 Wang, Q., Garrity, G.M., Tiedje, J.M., Cole, J.R., 2007. Naïve bayesian classifier for
802 rapid assignment of rRNA sequences into the new bacterial taxonomy. Appl.
803 Environ. Microbiol. 73, 5261-5267.
804 Wang, X.Z., Zhao, X.H., Li, H.B., Jia, J.L., Liu, Y.Q., Ejenavi, O., Ding, A.Z., Sun, Y.J.,
805 Zhang, D.Y., 2016. Separating and characterizing functional alkane degraders from
806 crude-oil-contaminated sites via magnetic nanoparticle mediated isolation. Res.
807 Microbiol. 167, 731-744.
808 Wentzel, A., Ellingsen, T.E., Kotlar, H.K., Zotchev, S.B., Throne-Holst, M., 2007.
809 Bacterial metabolism of long-chain n-alkanes. Appl. Microbiol. Biotechnol. 76,
810 1209-1221.
811 Widdel, F., Rabus, R., 2001. Anaerobic biodegradation of saturated and aromatic
812 hydrocarbons. Curr. Opin. Biotechnol. 12, 259-276.
813 Xi, H., Shen, J.L., Qu, Z., Yang, D.Y., Liu, S.M., Nie, X.H., Zhu, L.F., 2019. Effects of
814 long-term cotton continuous cropping on soil microbiome. Sci. Rep. 9, 18297.

Xia, X.F., Stewart, D.I., Cheng, L.R., Wang, K., Li, J., Zhang, D., Ding, A.Z., 2020a. Changes in groundwater bacterial community during cyclic groundwater-table variations. Hydrol. Process. 4, 1-12.

Xia, X.F., Cheng, L.R., Zhu, Y., Liu, Y.Q., Wang, K., Ding, A.Z., Cai, Z.S., Shi, H.S., Zuo, L.L., 2020b. Response of soil bacterial community and geochemical parameters to cyclic groundwater-level oscillations in laboratory columns. Vadose Zone J. 19, e20011.

Xiu, W., Lloyd, J., Guo, H.M., Dai, W., Nixon, S., Bassil, N.M., Ren, C., Zhang, C.R., Ke, T.T., Polya, D., 2020. Linking microbial community composition to hydrogeochemistry in the western Hetao Basin: potential importance of ammonium as an electron donor during arsenic mobilization. Environ. Int. 136, 105489.

Yakimov, M.M., Giuliano, L., Denaro, R., Crisafi, E., Chernikova, T.N., Abraham, W.R., Luensdorf, H., Timmis, K.N., Golyshin, P.N., 2004. *Thalassolituus oleivorans* gen. nov., sp. nov., a novel marine bacterium that obligately utilizes hydrocarbons. Int. J. Syst. Evol. Microbiol. 54, 141-148.

Yang, S.Z., Wen, X., Zhao, L., Shi, Y.L., Jin, H.J., 2014. Crude oil treatment leads to shift of bacterial communities in soils from the deep active layer and upper permafrost along the China-Russia crude oil pipeline route. Plos ONE 9, e96552.

Zhang, D., Cui, R.Y., Fu, B., Yang, Y.X., Wang, P.L., Mao, Y.T., Chen, A.Q., Lei, B.K., 2020. Shallow groundwater table fluctuations affect bacterial communities and

835 nitrogen functional genes along the soil profile in a vegetable field. Appl. Soil Ecol.
836 146, 103-368.
837 Zhou, Y.X., Kellermann, C., Griebler, C., 2012. Spatio-temporal patterns of microbial
838 communities in a hydrologically dynamic pristine aquifer. FEMS Microbiol. Ecol.
839 81, 230-242.
840 Zhu, H., Taylor, A.A., Astor, S.R., Terry, N., 2017. Enhancing saltgrass germination and
841 growth in a saline soil contaminated with petroleum hydrocarbons. Plant Soil 412,
842 189-199.

Figure captions

Fig. 1. (a) Schematic of the "vadose zone-fluctuating zone-saturated zone" continuum. (b) Schematic representation of the experimental timelines showing the sampling points. The grey (1) and dark red (1) and (2) shading represents the groundwater body in the static (ST) and rainfall infiltration (RI) columns when the sand samples were collected; orange line represents the intended pattern of water-table in the RI column.

Fig. 2. Changes in volumetric water content in the static (ST) and rainfall infiltration (RI) columns. V represents the vadose zone, F represents the fluctuating zone.

Fig. 3. Changes in dissolved oxygen in the static (ST) and rainfall infiltration (RI) columns. V represents the vadose zone, F represents the fluctuating zone, and S represents the saturated zone.

Fig. 4. Variation in n-alkane composition and concentration in the static (ST) and rainfall infiltration (RI) columns (the error bars represent the standard deviations of the mean values from triplicate measurements). V represents the vadose zone, F represents the fluctuating zone, and S represents the saturated zone; 1-6 represent the samples collected on days 20, 40, 90, 110,120 and 210, respectively.

864 **Fig. 5.** Variation in relative abundance of dominant phyla in the static (ST) and rainfall
865 infiltration (RI) columns. V represents the vadose zone, F represents the fluctuating zone,
866 and S represents the saturated zone; 1-6 represent the samples collected on days 20, 40,
867 90, 110,120 and 210, respectively.
868
869 **Fig. 6.** Variation in abundances of alkane monooxygenase genes in the static (ST) and
870 rainfall infiltration (RI) columns (the error bars represent the standard deviations of the
871 mean values from triplicate measurements). V represents the vadose zone, F represents
872 the fluctuating zone, and S represents the saturated zone; 1-6 represent the samples
873 collected on days 20, 40, 90, 110,120 and 210, respectively.
874
875 **Fig. 7.** Redundancy analysis (RDA) between environmental characteristics, n-alkane,
876 samples and bacterial communities at the phylum level. Grey circles and dark red stars
877 represent the static (ST) and rainfall infiltration (RI) columns, respectively. V represents
878 the vadose zone, F represents the fluctuating zone, and S represents the saturated zone;
879 1-6 represent the samples collected on days 20, 40, 90, 110,120 and 210, respectively.
880 Factors significantly impacted on bacterial community composition were marked with *
881 ($p < 0.05$) and ** ($p < 0.01$). WC: water content; DO: dissolved oxygen.

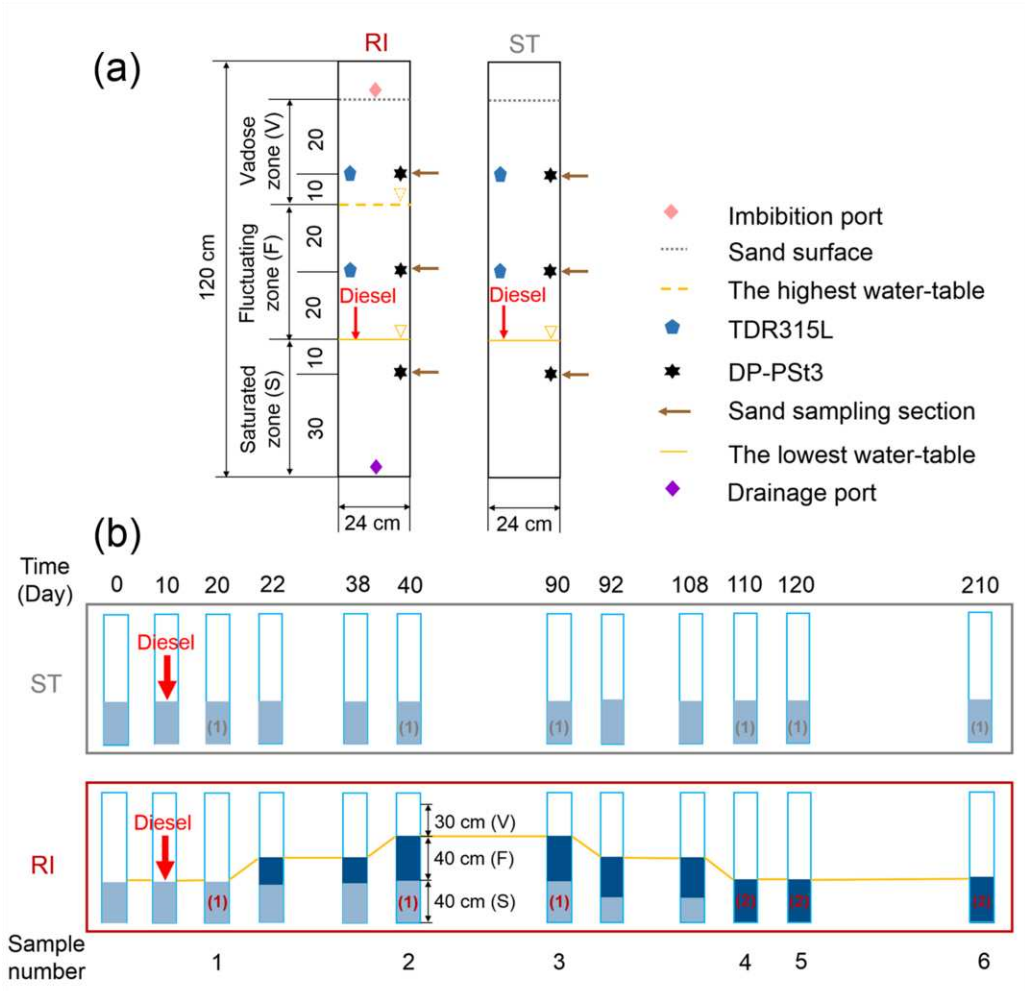

Fig. 1. (a) Schematic of the "vadose zone-fluctuating zone-saturated zone" continuum. (b) Schematic representation of the experimental timelines showing the sampling points. The grey (1) and dark red (1) and (2) shading represents the groundwater body in the static (ST) and rainfall infiltration (RI) columns when the sand samples were collected; orange line represents the intended pattern of water-table in the RI column.

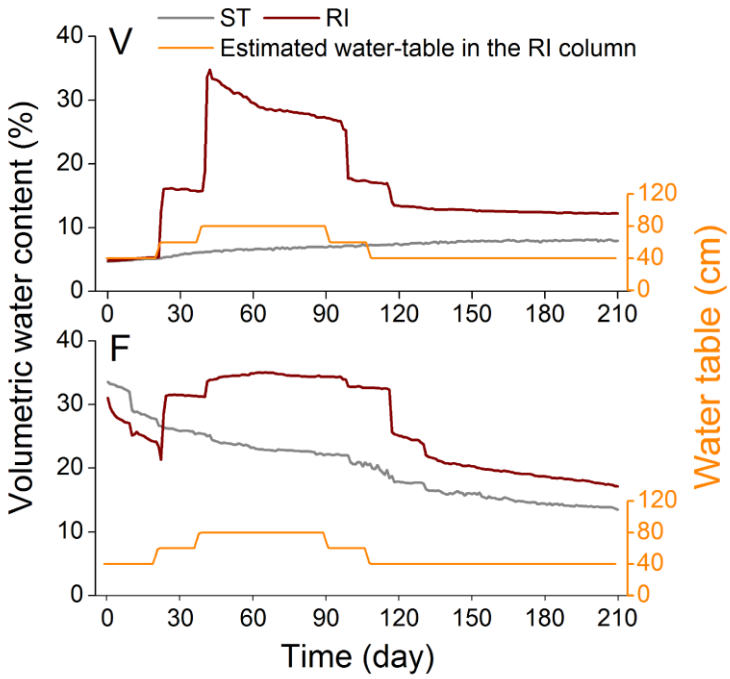

Fig. 2. Changes in volumetric water content in the static (ST) and rainfall infiltration (RI) columns. V represents the vadose zone, F represents the fluctuating zone.

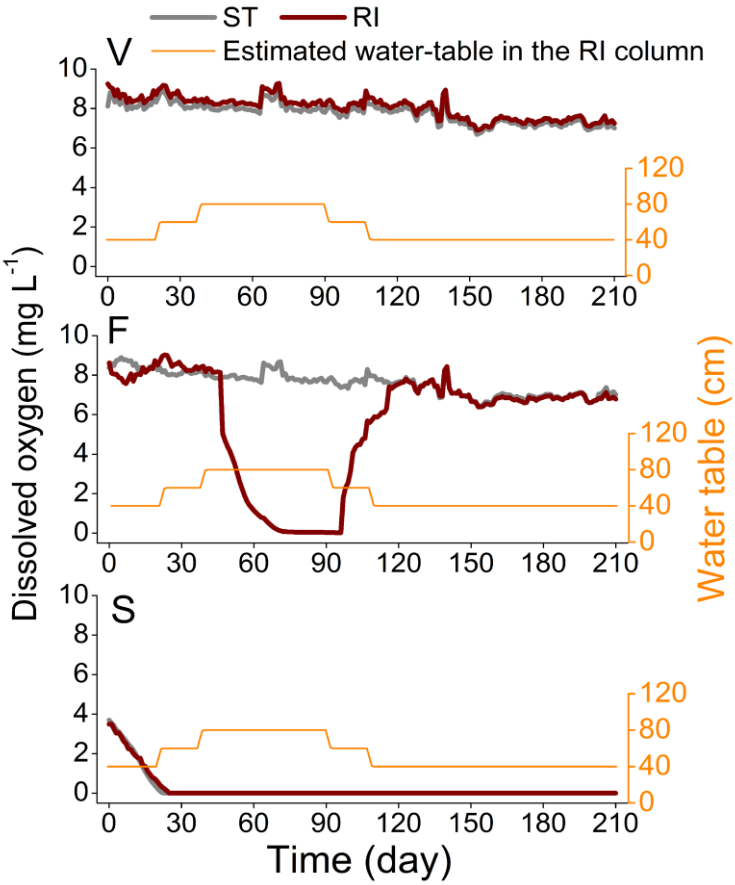

Fig. 3. Changes in dissolved oxygen in the static (ST) and rainfall infiltration (RI) columns. V represents the vadose zone, F represents the fluctuating zone, and S represents the saturated zone.

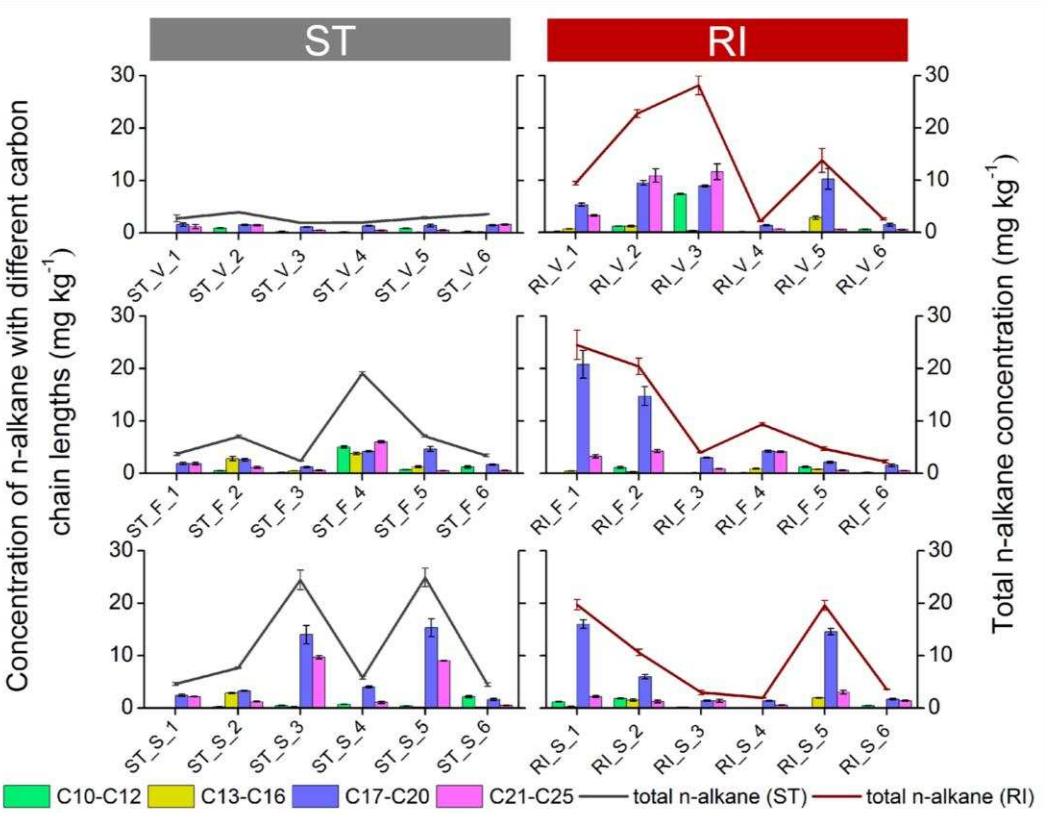

Fig. 4. Variation in n-alkane composition and concentration in the static (ST) and rainfall infiltration (RI) columns (the error bars represent the standard deviations of the mean values from triplicate measurements). V represents the vadose zone, F represents the fluctuating zone, and S represents the saturated zone; 1-6 represent the samples collected on days 20, 40, 90, 110,120 and 210, respectively.

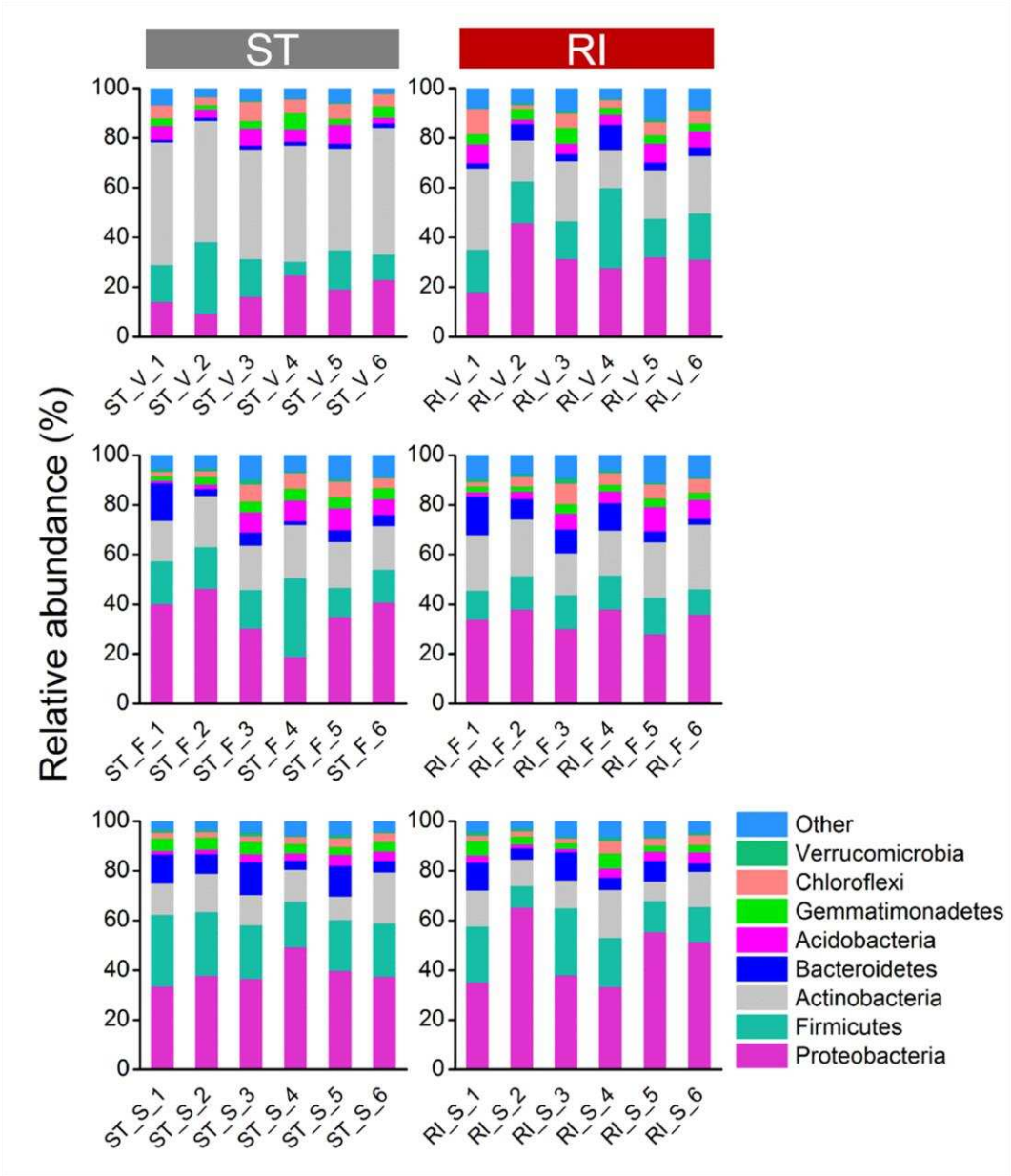

Fig. 5. Variation in relative abundance of dominant phyla in the static (ST) and rainfall infiltration (RI) columns. V represents the vadose zone, F represents the fluctuating zone, and S represents the saturated zone; 1-6 represent the samples collected on days 20, 40, 90, 110,120 and 210, respectively.

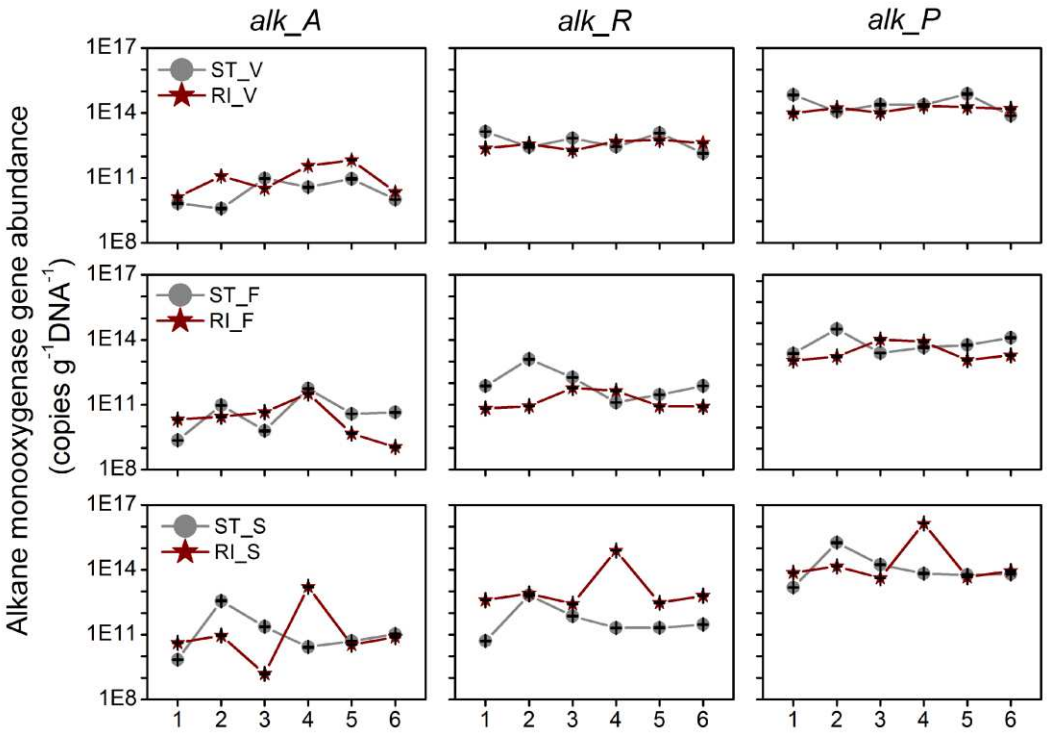

Fig. 6. Variation in abundances of alkane monooxygenase genes in the static (ST) and rainfall infiltration (RI) columns (the error bars represent the standard deviations of the mean values from triplicate measurements). V represents the vadose zone, F represents the fluctuating zone, and S represents the saturated zone; 1-6 represent the samples collected on days 20, 40, 90, 110,120 and 210, respectively.

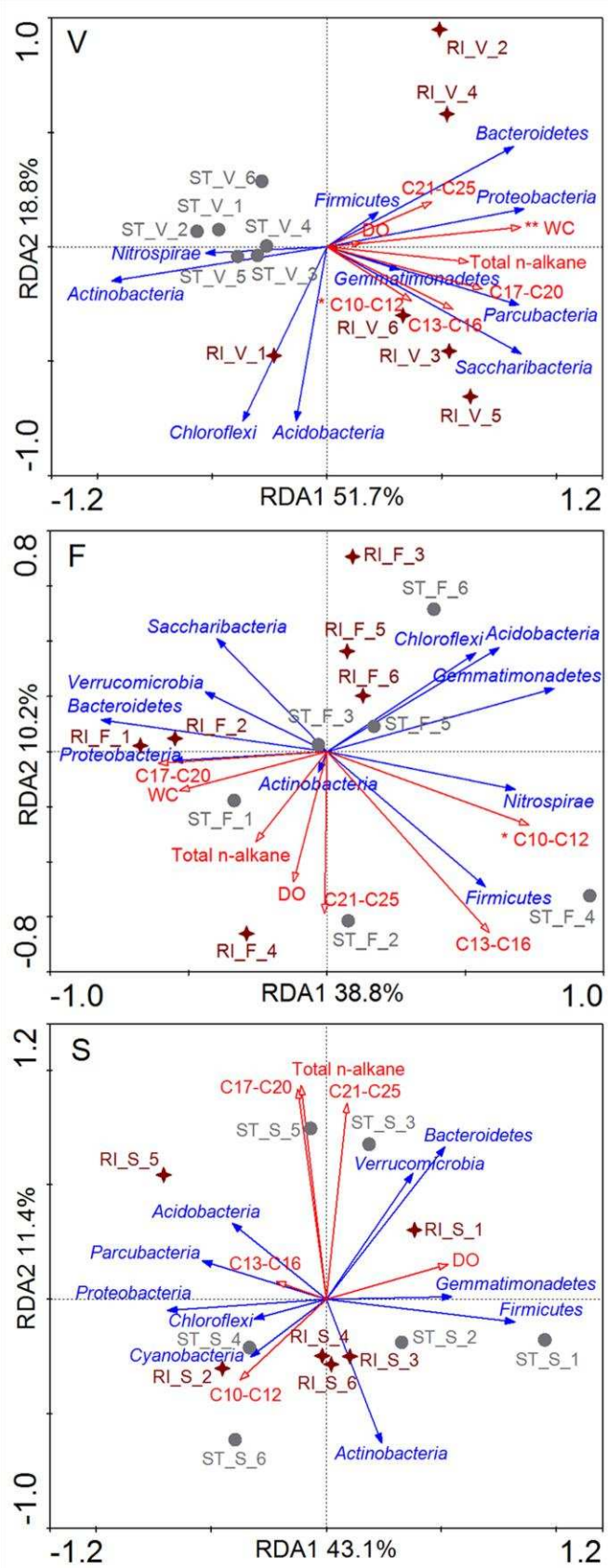
V
RI_V_2
RI_V_4
Bacteroidetes
ST_V_6
ST_V_1
ST_V_2
ST_V_4
Firmicutes
C21-C25
Proteobacteria
DO
** WC
Nitrospirae
Total n-alkane
ST_V_5
ST_V_3
Gemmatimonadetes
C17-C20
Actinobacteria
* C10-C12
Parcubacteria
RI_V_6
C13-C16
RI_V_1
RI_V_3
Saccharibacteria
RI_V_5
Chloroflexi
Acidobacteria
1.0
-1.0
RDA2 18.8%
-1.2
RDA1 51.7%
1.2
F
RI_F_3
ST_F_6
Saccharibacteria
RI_F_5
Chloroflexi
Acidobacteria
RI_F_6
Gemmatimonadetes
Verrucomicrobia
Bacteroidetes
ST_F_3
ST_F_5
RI_F_2
RI_F_1
Proteobacteria
C17-C20
WC
Actinobacteria
Nitrospirae
ST_F_1
* C10-C12
Total n-alkane
DO
C21-C25
Firmicutes
ST_F_4
ST_F_2
C13-C16
RI_F_4
0.8
-0.8
RDA2 10.2%
-1.0
RDA1 38.8%
1.0
S
Total n-alkane
C17-C20
C21-C25
ST_S_5
ST_S_3
Bacteroidetes
RI_S_5
Verrucomicrobia
Acidobacteria
RI_S_1
Parcubacteria
C13-C16
DO
Proteobacteria
Gemmatimonadetes
Chloroflexi
Firmicutes
ST_S_4
RI_S_4
ST_S_2
Cyanobacteria
RI_S_3
ST_S_1
RI_S_2
C10-C12
RI_S_6
ST_S_6
Actinobacteria
1.2
-1.0
RDA2 11.4%
-1.2
RDA1 43.1%
1.2

914

915 **Fig. 7.** Redundancy analysis (RDA) between environmental characteristics, n-alkane, samples
916 and bacterial communities at the phylum level. Grey circles and dark red stars represent the static
917 (ST) and rainfall infiltration (RI) columns, respectively. V represents the vadose zone, F
918 represents the fluctuating zone, and S represents the saturated zone; 1-6 represent the samples
919 collected on days 20, 40, 90, 110,120 and 210, respectively. Factors significantly impacted on
920 bacterial community composition were marked with * ($p < 0.05$) and ** ($p < 0.01$). WC: water
921 content; DO: dissolved oxygen.

Highlights

n-Alkanes (LNAPLs) move vertically in an aquifer with water table variations

RDA revealed key factors affecting bacterial community variation in different zones

The water table moderated moisture-niche selection for subsurface bacteria

Gene for n-alkane degradation (*alkB*) is common in subsurface bacterial populations

Variations in water table cause transitory increases in abundance of the *alkB* gene